

GaAs/AlGaAs SURFACE EMITTING LASER DIODE WITH VERTICAL DISTRIBUTED FEEDBACK OPTICAL CAVITY AND TRANSVERSE JUNCTION BURIED HETEROSTRUCTURE

Wei Hsin, Mutsuo Ogura^{a)}, Jean-Pierre Weber, S.C. Wang^{b)}, J.J. Yang^{c)},
M.C. Wu, Shyh Wang, and John R. Whinnery.

Department of Electrical Engineering and Computer Science, and
Electronics Research Laboratory, University of California, Berkeley, CA 94720

ABSTRACT

A threshold current of 2 mA at room temperature CW operation is realized in a vertical distributed feedback surface emitting laser diode (VDFB-SELD) with transverse junction buried heterostructure (TJBH). In this TJBH structure, the vertical distributed feedback active region (AlGaAs/GaAs multilayer) is entirely surrounded by N- and P-type AlGaAs cladding layer for minority carrier confinement. The far field angle is 7 to 8 degrees. The beam shape is nearly circular. However, the lasing spectrum is broad (1.5 to 3 nm) compared with the conventional edge-emitting laser. Theoretical model of the VDFB-SELD-TJBH by using DFB theory and its computer simulation of the spectrum shows good agreement with the experimental measurements.

INTRODUCTION

The vertical distributed feedback surface emitting laser diode (VDFB-SELD) is very advantageous for optoelectronic integration because it does not need cleavage nor a backside substrate etching process to form a vertical optical cavity [1,2]. High reflectivity of the cavity mirrors and high efficiency in the carrier confinement structure are important to realize low threshold current operation of the VDFB-SELD. High reflectivity of the cavity mirrors was already realized by the use of a quarter wavelength stack of AlGaAs and GaAs thin layers [3]; however, carrier confinement was not adequate in the previous structures [1,2]. In this report, we realized a novel transverse junction buried heterostructure (TJBH) by selective liquid phase epitaxy (LPE) and selective zinc diffusion, and achieved a room-temperature, low-threshold current, CW operation of the VDFB-SELD.

DEVICE FABRICATION

Figure 1 depicts the VDFB-SELD-TJBH structure. The active layer is made of a quarter wavelength stack of $Al_{0.3}Ga_{0.7}As$ and GaAs thin layers prepared by metal-organic chemical vapor deposition (MOCVD). The thicknesses of each pair of AlGaAs/GaAs layers are first chosen and then adjusted so that the reflectivity is peaked near the gain maximum of GaAs. The optical cavity, formed by these AlGaAs/GaAs multilayers, consists of 20

a) also with Electrotechnical Laboratory, Sakura-mura, Niihari-gun, Ibaraki 305 Japan b) Research & Development Division, Lockheed Missiles & Space Company, Inc., Palo Alto, CA 94304-1187 c) Space and Technology Group, TRW, One Space Park, Redondo Beach, California 92078

pairs at the top, 60 pairs at the bottom, and a phase shifter GaAs layer in between. The thickness of the GaAs phase shifting layer is about half wavelength of the gain maximum, which allows the laser to lase at the Bragg wavelength of the multilayer. This multilayer is etched by a wet etching solution leaving mesas with different dimensions ranging from 2×8 to $3 \times 17 \mu m$ on the top surface and $10 \mu m$ in height with the DFB type active region. The N-type $Al_{0.4}Ga_{0.6}As$ cladding layer is formed by selective LPE using silicon nitride on top of the mesa as a selective epitaxial mask. The lateral pn-junction is formed by selective zinc diffusion through an opening in the silicon nitride film at a distance of 3 to $4 \mu m$ away from the edge of the mesa. Due to lateral diffusion, the zinc diffusion front is inside the multilayer. In this structure, the GaAs/AlGaAs part of the multilayer is completely surrounded by the N- or P-type AlGaAs. Therefore, carrier confinement should be comparable with that of buried hetero-structures used with the edge emitting laser diode. The zinc diffusion front spreads along the cladding region as well as along the AlGaAs/GaAs multilayer. However, carriers are injected predominantly into the GaAs part of the multilayer because the turn-on voltage for an AlGaAs pn-junction is higher than for a GaAs pn junction.

DEVICE RESULTS

Figure 2 shows the light output versus dc current (L-I) characteristics of the VDFB-SELD. The laser is operated CW at room temperature. The threshold current is 2 mA as seen in the inset of this figure. The total light output increases linearly up to 25 mA. The output power is $28 \mu W$ at 10 mA and $87 \mu W$ at 25 mA.

Figure 3(a) shows the near-field pattern of the VDFB-SELD. The light-emitting region is tightly confined within the rectangular top emission surface. Therefore, carrier confinement by the TJBH structure is very effective. Figure 3(b) shows the far-field pattern at an operating current of 20 mA. It shows a nearly circular pattern with a gaussian-like intensity profile. The estimated beam divergence angle is about 7 to 8 degrees. This indicates a good spatial coherence in this device. However, the circular emission pattern is not expected from a trapezoidal mesa cavity with a rectangular emission surface. We think that the curved boundary between the AlGaAs/GaAs multilayer active region and AlGaAs cladding region may affect the emission beam pattern.

Figure 4 shows the CW electroluminescence spectra

of the VDFB-SELD-TJBH structure. As is seen in the inset of the figure, the onset of sharp emission line at 884 nm becomes obvious at the drive current of 1.6 mA. This current level is consistent with the threshold current deduced from the L-I characteristics. The half width of the lasing spectrum at 884 nm is rather wide (1.5 to 3 nm) compared with an edge-emitting (EE) laser diode and there is a large amplified spontaneous emission at the shorter wavelength side. However, there are fundamental differences between the short-cavity SE and long-cavity EE lasers. First, the mode spacing in the SE laser is much wider than the EE laser. For such wide spectral separation, the mode broadening mechanism will be different from that of the EE laser. Second, the spontaneous emission factor in the short-cavity SE laser is expected to be much larger than that in the long-cavity EE laser [4]. Both these factors will affect the behavior of the two types of lasers in terms of lasing spectrum.

THEORETICAL MODELING OF DEVICE

We use Bloch wave theory for the DFB multilayer section [5] and consider the laser as an amplifier driven by spontaneous emission. Figure 5 shows the idealized structure we used for the calculation of the reflectivity curve and emission spectrum. E_1 & E_4 , E_2 & E_3 are the electric fields of the forward- and backward-going waves respectively, at the two interfaces of the phase shifter region (L_3). S_i 's are the equivalent sources at the interfaces due to the random spontaneous emission in each section. R_i 's and T_i 's are the reflection and transmission coefficients of the Bloch waves at the interfaces. R_2 , R_3 and T_2 , T_3 refer to the phase shifter as a whole. The round-trip condition is given by:

$$(1 - R_1 R_2 P_2^2)(1 - R_3 R_4 P_4^2) = R_1 R_4 T_2 T_3 P_2^2 P_4^2 \quad (1)$$

where the P_i 's are the propagation factors in each section [5]. From Eqn.(1), we can calculate the wavelengths and threshold gains of the modes. The output spectral power density is given by:

$$P_{out}(\lambda) = \left| R_1 T_1 P_2 \frac{N}{D} + T_1 \right|^2 P_1(\lambda) + \left| T_1 P_2 \frac{N}{D} \right|^2 P_2(\lambda) + \left| T_1 P_2 \frac{T_3}{D} \right|^2 P_3(\lambda) + \left| T_1 T_3 R_4 P_2 \frac{P_4}{D} \right|^2 P_4(\lambda) \quad (2)$$

where

$$N = R_2 + R_4 P_4^2 (T_2 T_3 - R_2 R_3)$$

$$D = (1 - R_1 R_2 P_2^2)(1 - R_3 R_4 P_4^2) - R_1 R_4 T_2 T_3 P_2^2 P_4^2$$

and the $P_i(\lambda)$'s are the spectral power densities of the equivalent spontaneous emission sources S_i 's at the four interfaces. Realistic gain and spontaneous emission spectrum were used for the calculations.

COMPUTER SIMULATION RESULTS

Figure 6 shows the reflectivity curve measured from the top surface and the theoretical calculation based on Bloch wave theory. The agreement is very good in predicting the shape of reflectivity curve. Figure 7 shows the experimental pulsed spectrum and the computer calculated power spectrum from Eqn.(1) and Eqn.(2) above, at

different carrier densities. The agreement is fairly good. The lowest effective threshold power gain mode ($G_{th} \sim 3.6 \text{ cm}^{-1}$) is at 884 nm from calculation, all the other modes which appear as the humps in the spectrum have a much higher effective threshold power gain ($G_{th} \sim 1.2 \times 10^3 \text{ cm}^{-1}$). Thus, only the mode at 884 nm is lasing (i.e. above threshold), all the other modes are still below threshold at these current levels. Therefore, the emission spectrum shows a sharp peak at 884 nm and much broader humps at shorter wavelengths due to the amplified spontaneous emission produced by these high threshold gain modes. In this model, we assume that the carrier density is given and the gain spectrum is then calculated with a semi-empirical model, assuming Fermi-Dirac distributions in the bands. Gain saturation is not taken into account. Therefore, the model is really valid only below threshold and fails to give the exact amplitude of the lasing peak above threshold. The fact that it reproduces the shape of the spectrum above threshold elsewhere indicates that there is inhomogeneous broadening and that the carrier density is not clamped at threshold. The measured FWHM of the lasing peak is probably larger than the real one because of the limited resolution (7 Å) of the measurement (which was incorporated in the simulations).

CONCLUSIONS

In conclusion, the VDFB-SELD-TJBH structure is realized with the combination of MOCVD, selective LPE, and zinc diffusion techniques. In this structure, an MOCVD-grown AlGaAs/GaAs multilayer is surrounded completely by P- and N-type AlGaAs cladding layers, such that lateral carrier injection and carrier confinement are achieved. Nominal threshold current for CW operation is 2 mA. The radiation region is well confined within the active region. The far-field pattern is circular and well defined. However, lasing spectra at 884 nm is broad (1.5 to 3 nm) and there is large amplified spontaneous emission at shorter wavelengths. Computer simulation shows good agreement with the measurement. Further improvement of the spectrum can be realized by proper modifications of the optical cavity and layer thickness of the multilayer and phase shifter.

ACKNOWLEDGEMENTS

The authors acknowledge contributions of Dr. Shih-Yuan Wang and Yu-Min Houg of Hewlett Packard Laboratory, Palo Alto; and Dr. Michael Rubin of Lawrence Berkeley Laboratory. They also acknowledge Professor A.E. Siegman of Stanford University; Professor A. Dienes of the University of California, Davis; Professor J.S. Smith, and Ghulam Hasnain of the University of California, Berkeley; and T.R. Ranganath of Hewlett Packard Laboratory, Palo Alto, for their helpful discussions. They also appreciate the technical assistance of Lillian Z. Gacusan, and Larry Dries of the Lockheed Missiles & Space Company, Inc., Palo Alto. This work is supported in part by NSF No. ECE-8410838, JSEP No.F49620-84-C-0057, Lockheed Missiles & Space Company, and the Office of Naval Research.

REFERENCES

- [1]. M. Ogura, S. Mukai and S. Wang, Proc. of the device research conference, May 1986
- [2]. M. Ogura, T. Hata, and T. Yao, Jpn. J. Appl. Phys.

- [3]. M. Ogura, T. Hata, N.J. Kawai, and T.Yao, Jpn. J. Appl. Phys. 22, (1983) L112
- [4]. T.P. Lee, C.A. Burrus, J.A. Copeland, A.G. Dentai, and D. Marcuse, IEEE J. Quantum Electron, QE-18, 1101 (1982)
- [5]. Shyh Wang, *Semiconductors and Semimetals*, Vol. 22 Part E, Chap 1., Academic Press, Inc., 1985.

FIGURE CAPTIONS

- Fig.(1) (a)Schematic diagram of the VDFB-SELD-TJBH structure. (b)Cross-sectional SEM picture of the VDFB-SELD-TJBH structure. The white contrasted region at the right side of the multilayer is a zinc diffused P-type AlGaAs cladding layer.
- Fig.(2) Light output versus dc drive current of the VDFB-SELD-TJBH structure.
- Fig.(3) (a)Near-field pattern of the VDFB-SELD. Also shows the line profile of the field intensity across the long edge of the rectangular emission region. (b)Far-field pattern and its intensity line profile across the beam center of the VDFB-SELD.
- Fig.(4) CW electroluminescence spectra of the VDFB-SELD.
- Fig.(5) Schematic diagram of the idealized VDFB-SELD structure used for theoretical model. L_3 is the phase shifter region, L_2 & L_4 & L_5 are the multilayer DFB section.
- Fig.(6) Measured and calculated reflectivity curve of the multilayer from the top surface.
- Fig.(7) Spectrum of the VDFB-SELD. (a)Experimental measurements (400 ns pulse). Resolution of the monochromator is 0.7 nm in the measurement. (b)Computer simulation results for carrier density $N=0.5 \times 10^{18} \text{ cm}^{-3}$ (1), $1 \times 10^{18} \text{ cm}^{-3}$ (2), $2 \times 10^{18} \text{ cm}^{-3}$ (3), $3 \times 10^{18} \text{ cm}^{-3}$ (4).

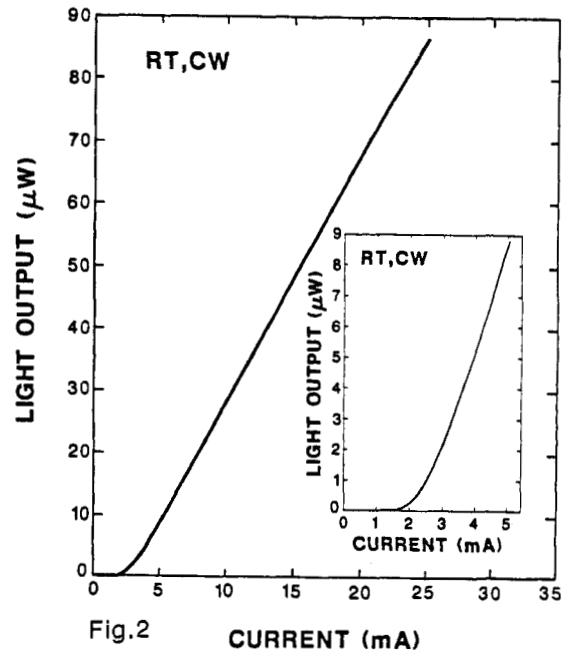
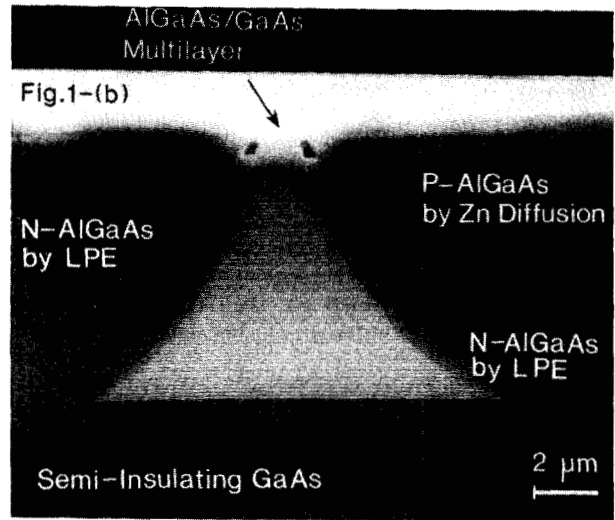
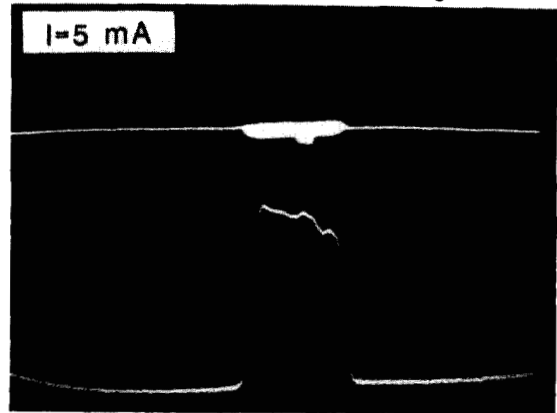
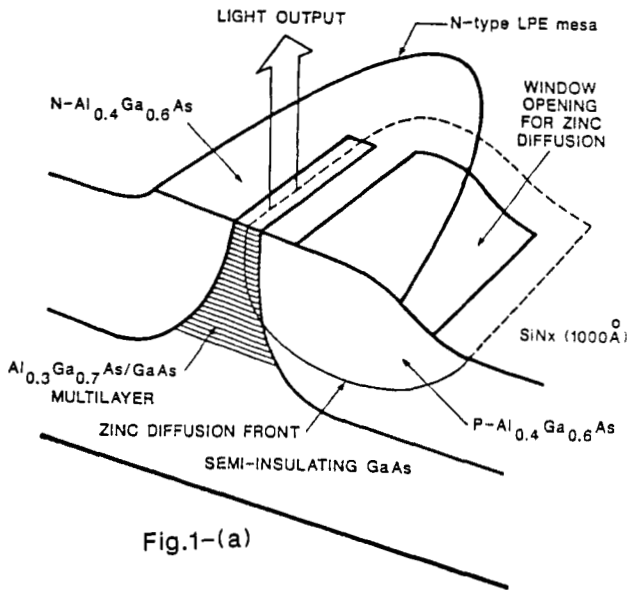


Fig.2
CURRENT (mA)
NEAR FIELD

Fig.3-(a)



FAR FIELD Fig.3-(b)

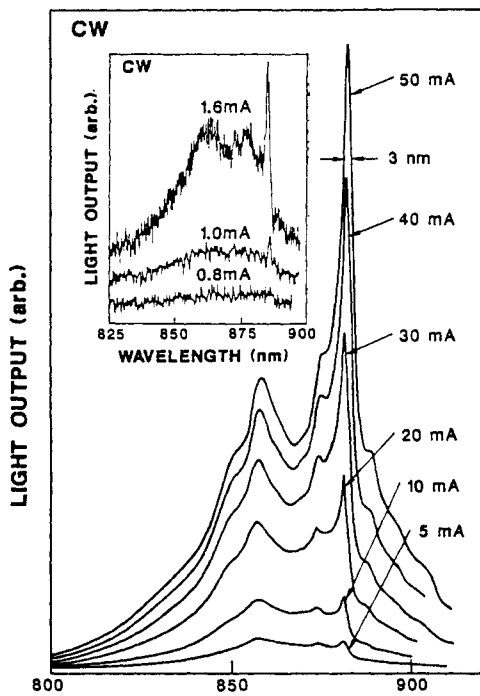
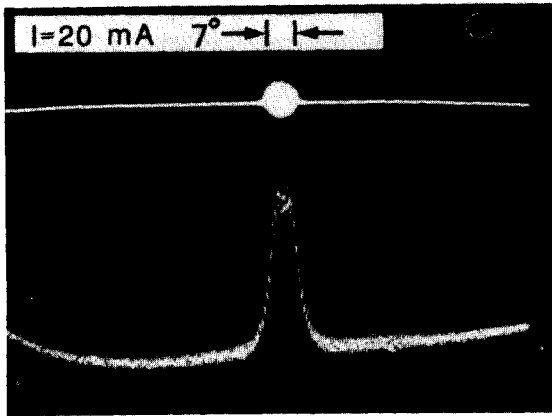


Fig.4 Wavelength (nm)

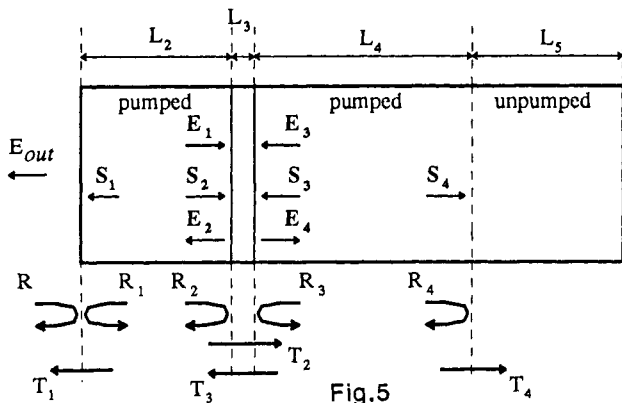


Fig.5

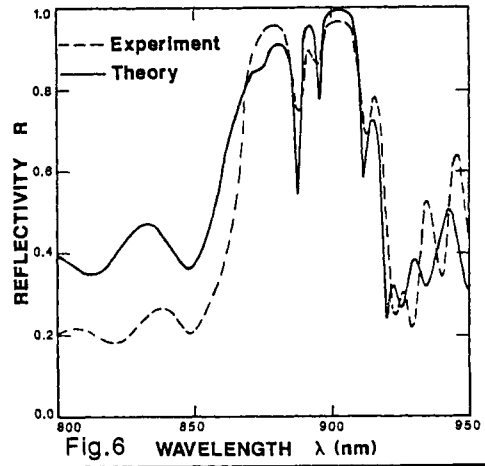


Fig.6 Wavelength λ (nm)

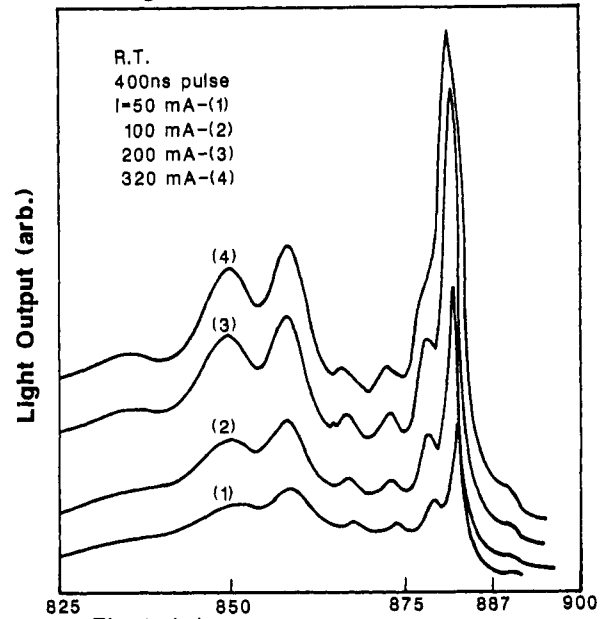


Fig.7-(a) Wavelength (nm)

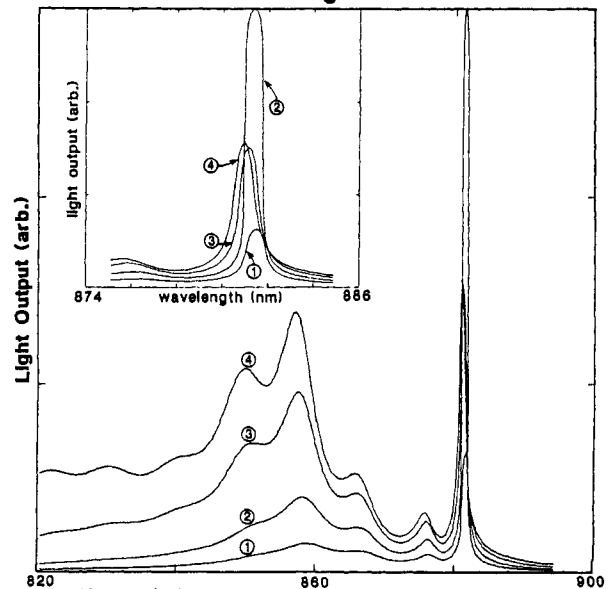
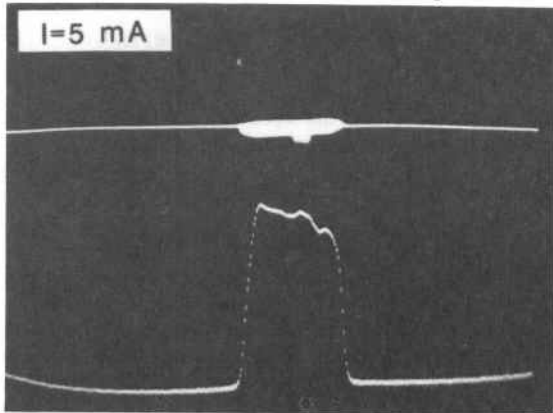


Fig.7-(b) Wavelength (nm)

NEAR FIELD

Fig.3-(a)



FAR FIELD

Fig.3-(b)

